Korean J. Chem. Eng., 33(3), 755-763 (2016)
DOI: 10.1007/s11814-015-0195-7

pISSN: 0256-1115
eISSN: 1975-7220

Development of an optimal multifloor layout model for the generic liquefied natural gas liquefaction process

Jin-Kuk Ha and Euy Soo Lee†

Department of Chemical and Biochemical Engineering, Dongguk University,
30, Pildong-ro 1-gil, Jung-gu, Seoul 04620, Korea
(*Received 12 December 2014 • accepted 9 September 2015*)

Abstract−Liquefied natural gas (LNG) is attracting significant interest as a clean energy alternative to other fossil fuels, mainly for its ease of transport and low carbon dioxide emission. As worldwide demand for LNG consumption has increased, liquefied natural gas floating, production, storage, and offloading (LNG-FPSO) operations have been studied for offshore applications. In particular, the LNG-FPSO topside process systems are located in limited areas. Therefore, the process plant layout of the LNG-FPSO topside systems will be optimized to reduce the area cost occupied by the topside equipment, and this process plant layout will be designed as a multifloor concept. We describe an optimal layout for a generic offshore LNG liquefaction process operated by the dual mixed refrigerant (DMR) cycle. To optimize the multifloor layout for the DMR liquefaction cycle process, an optimization was performed by dividing it into first and the second cycles. A mathematical model of the multifloor layout problem based on these two cycles was formulated, and an optimal multifloor layout was determined by mixed integer linear programming. The mathematical model of the first cycle consists of 725 continuous variables, 198 equality constraints, and 1,107 inequality constraints. The mathematical model of the second cycle consists of 1,291 continuous variables, 286 equality constraints, and 2,327 inequality constraints. The minimization of the total layout cost was defined as an objective function. The proposed model was applied to DMR liquefaction cycle process to determine the optimal multifloor layout.

Keywords: Process Plant Layout, MILP, Optimization, Dual Mixed Refrigerant Cycle

INTRODUCTION

As global energy consumption is gradually increasing, liquefied natural gas (LNG) is attracting significant interest as the cleanest energy source among the fossil fuels, mainly for its ease of transport and low carbon dioxide emission, a primary factor in air pollution and global warming [1]. For this reason, liquefied natural gas floating, production, storage, and offloading (LNG-FPSO) operations have been studied in extensive detail [1,2]. The LNG-FPSO systems consist of a hull, turret, and topside. The topside is divided into the LNG liquefaction process and utility system. The LNG liquefaction process consists of the separation, pretreatment, and liquefaction processes, and can be classified as mixed refrigerant (MR) liquefaction cycle, dual mixed refrigerant (DMR) liquefaction cycle, cascade liquefaction, and propane precooled mixed refrigerant liquefaction cycle. In particular, the LNG liquefaction process is important in the LNG-FPSO topside process and typically accounts for 70% of the capital cost of the topside process system and 30-40% of the overall plant cost [18,21]. Moreover, LNG-FPSO topside process systems are located in a limited area. Therefore, this process plant layout will be optimized to reduce the area occupied by the topside equipment at the front-end engineering design stage, and the process plant layout of the LNG-FPSO topside equipment will be designed as multifloor instead of a single floor [3].

The problem of process layout and location is relatively old and has received considerable attention over the years in the field of operational research. The optimal decision on the process plant layout concerning the allocation of equipment items and the required connections among them during the design of a plant may reduce construction, land area and operating costs, and increase the safety of the plant [4,6,7]. A number of different approaches have been considered for the process plant layout problem. Heuristic techniques were suggested at first, offering computational efficiency, but there is no guarantee on the optimality of the solution [5,13]. The use of the genetic algorithms proved to be effective in obtaining good and practical solutions for the layout problem [10]. The optimization-based techniques have also been presented. A mixed integer nonlinear programming (MINLP) model was proposed by Penteado and Ciric [12], accounting for the financial risk associated with accidents and their propagation to neighboring units, as well as incorporating other terms such as piping and land and protection device costs. Continuous domain MILP mathematical models were presented by Papageorgiou and Rotstein [11], determining simultaneously optimal location and orientation for each equipment item to minimize a given performance criterion. The MILP model was then generalized to account for the organization of the process plant layout into the production sections. An alternative continuous MILP formulation was suggested by Ozyruth and Realff [17] for equipment allocation, utilizing a piecewise-linear function representation for absolute the value functional to determine the

†To whom correspondence should be addressed.
E-mail: eslee@dongguk.edu

distances between the equipment items. Georgiadis et al. suggested that the MLIP model must be minimized to account for the total transport, connection, land and floor construction cost. Moreover, Park et al. suggested an MILP formulation to optimize plant layout in a multifloor facility including land and floors area cost, piping and pumping costs, as well as the expected loss caused by equipment explosions [16].

In the LNG liquefaction process, many liquefaction processes have been developed and used over the last few decades. The optimal operational conditions and synthesis of various LNG liquefac-

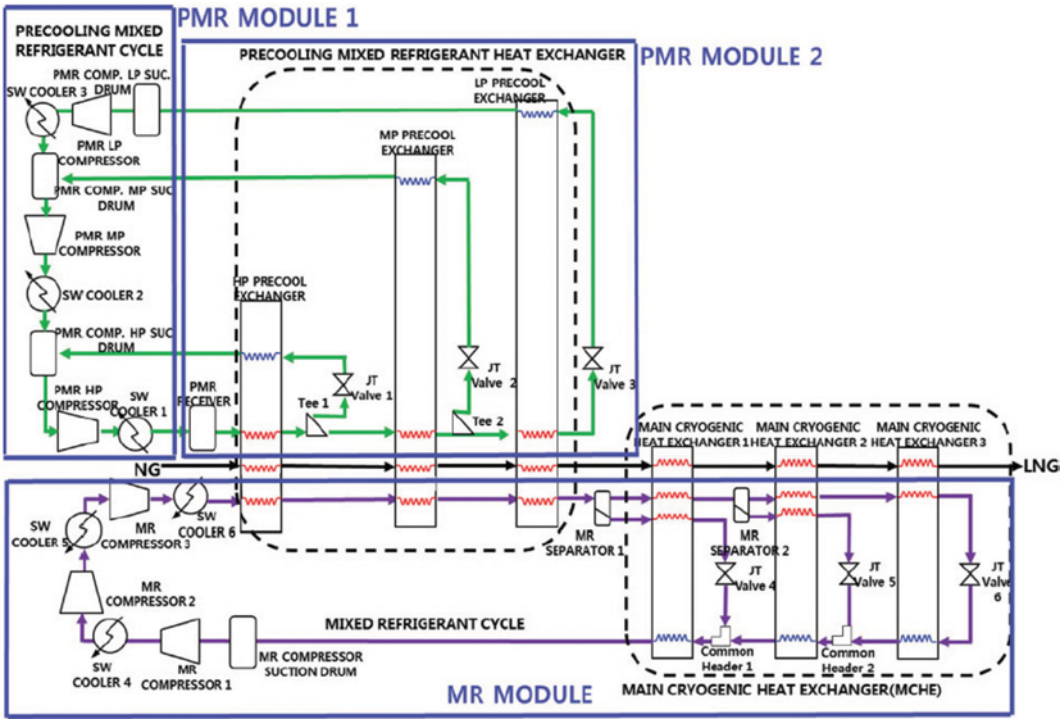

Fig. 1. The MR liquefaction cycle process.

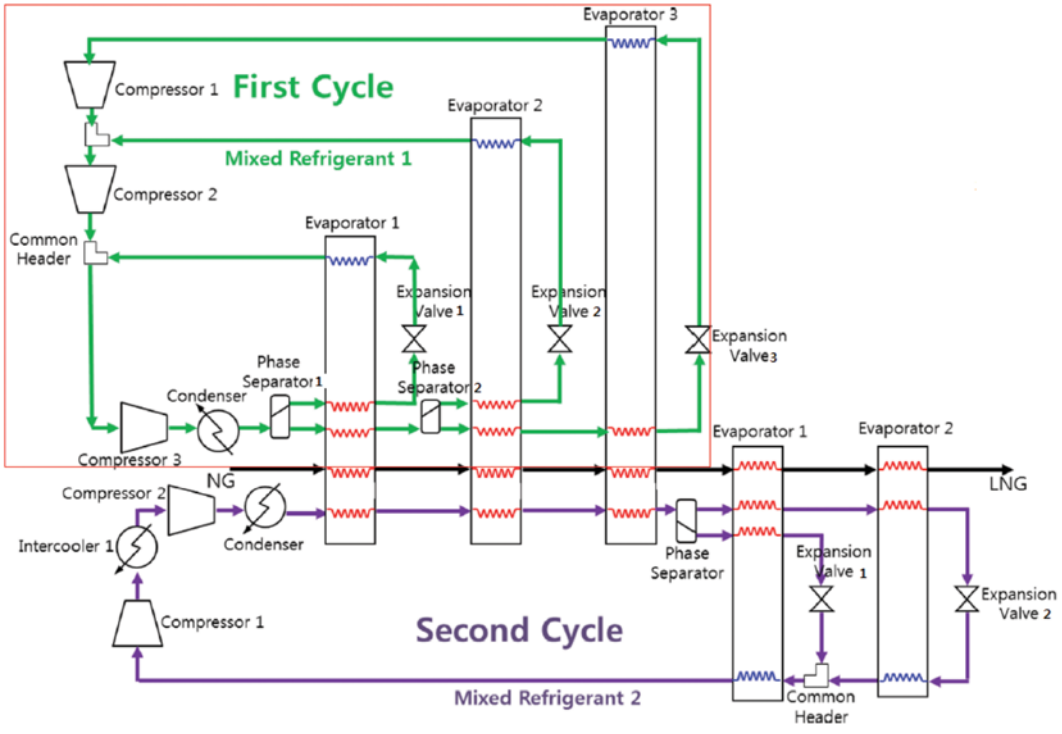

Fig. 2. The DMR liquefaction cycle process.

tion process cycles have been studied. However, the optimal layout problem in the LNG liquefaction process cycle process has been studied in recent years. Ku et al. proposed the optimal module layout for a multifloor MR liquefaction cycle process, considering safety. In addition, the optimal solution of this plant was determined using the MINLP model [19,20]. As shown in Fig. 1, the MR liquefaction cycle process is divided into three modules: MR, PMR1, and PMR2 modules. Ku et al. performed the optimization by dividing it into the three modules [19]. In this case, because the MR liquefaction cycle process is divided into several parts, the connection between the equipment and equipment among each module was not considered. Therefore, for satisfying the distance constraint between the equipment and equipment among each module and optimizing the distance constraint for the entire process, the connection for between equipment and equipment among each part should be considered. This consideration can satisfy the distance constraint between the equipment items and optimize the distance constraint for the entire process, when the optimal layout of each module is determined.

In this study, we describe an optimal multifloor layout of the DMR liquefaction cycle for the generic offshore LNG liquefaction process, as shown in Fig. 2. The number of the floors, land area, floor allocation of each equipment item and detailed layout for the DMR liquefaction cycle was determined using mixed integer linear programming (MILP) proposed by Patsiatzis and Papageorgiou [14]. A mathematical model of the multifloor layout problem for the process of the DMR liquefaction cycle is formulated. Moreover, as shown in Fig. 2, three evaporators in the first cycle are connected to the second cycle. Therefore, for satisfying the distance constraint between the equipment and the equipment among each cycle and optimizing the distance constraint for the entire process, we assumed that three evaporators in the first cycle exist in the second cycle. To minimize the disconnection between the equipment and the equipment among each cycle, an optimization was performed by dividing into the first and the second cycles.

1. Generic LNG Liquefaction Process

The generic LNG liquefaction process is limited to the dual cycle to implement offshore applications, as shown in Figs. 1 and 2. The reasons for limiting the model to the dual cycle are as follows: the DMR cycle is now being considered for the applications in LNG-FPSO, and the propane-precooled mixed refrigerant cycle is one of the most commonly used systems for onshore applications, along with the dual cycle [2]. Therefore, the dual cycle is considered to be the generic LNG liquefaction process for the offshore applications in terms of reliability. Moreover, the maximum number available for each main piece of equipment (compressor, expansion valve, condenser, and evaporator) is three per cycle, taking into account offshore requirements such as the compactness (related to energy efficiency), motion effects, and process plant layout [1-3]. As shown in Fig. 2, precooling and main cooling occur in the first and second cycles, respectively, to completely liquefy the natural gas. The DMR liquefaction cycle process is a high-pressure system using compressors [2,3]. The approximate size of the abovementioned equipment is shown in Tables 1 and 2, if this DMR liquefaction capacity is assumed to be in the range 479-500 kg/h (4.0 million tons per year) [2,19,20].

Table 1. Dimensions of the equipment in the first cycle of the DMR liquefaction cycle process

No.	Name of equipment	α_i (m)	β_i (m)	h_i
1, 2, 3	Evaporator 1	4	4	21
4, 5, 6	Evaporator 2	5	5	23
7, 8, 9	Evaporator 3	4	4	22
10	Expansion valve 1	1	1	N/A
11	Expansion valve 2	1	1	N/A
12	Expansion valve 3	1	1	N/A
13	Phase separator 1	3	3	9
14	Phase separator 2	3	3	9
15	Condenser	4	6	5
16	Compressor 1	4	4	5
17	Compressor 2	4	4	5
18	Compressor 3	4	4	5

Table 2. Dimensions of the equipment in the second cycle of the DMR liquefaction cycle process

No.	Name of equipment	α_i (m)	β_i (m)	h_i
1, 2, 3	Evaporator 1 (first cycle)	4	4	21
4, 5, 6	Evaporator 2 (first cycle)	5	5	23
7, 8,9	Evaporator 3 (first cycle)	4	4	22
10, 11, 12, 13, 14	Evaporator 1 (second cycle)	3	3	42
15, 16, 17, 18, 19	Evaporator 2 (second cycle)	3	3	42
20	Expansion valve 1	1	1	N/A
21	Expansion valve 2	1	1	N/A
22	Phase separator 1	3	3	9
23	Condenser	4	6	5
24	Compressor 1	4	4	5
25	Compressor 2	4	4	5
26	Intercooler 1	5	2	5

The generic LNG liquefaction process has been used in the DMR cycle, as shown in Fig. 2. Therefore, to optimize the multifloor layout for the generic offshore LNG liquefaction process, an optimization was performed by dividing into the first and the second cycles and considering the safety and the distance between the equipment items. The plant layout was also optimized based on the MILP model proposed by Patsiatzis and Papageorgiou [14].

2. Mathematical Formulation for the Optimal DMR Cycle Process Layout

In the formulation presented here, rectangular shapes were assumed for the equipment items following the current industrial practices. The rectilinear distances between the equipment items are used for a more realistic estimate of the piping costs [12,14]. Equipment items, which are allowed to rotate 90°, were assumed to be connected through their geometrical centers.

2-1. Floor and Equipment Orientation Constraints

When applied to all the equipment on the DMR liquefaction cycle process, each equipment item should be assigned to one floor, and this can be expressed as follows:

$$\Sigma_{k=1}^{NF} V_{ik} = 1 \quad \forall i \tag{1}$$

Number of floors NF=4 (the first cycle), 5 (the second cycle), and the height between floors H=10 m.

If the height of the equipment exceeds the height of a floor, (H=10 m), the equipment should be installed across two or more floors. Accordingly, if one equipment will be installed across two floors, the number of this equipment is two.

For the first cycle

$$\Sigma_{k=1}^{4} V_{ik}=1 \quad i=1, 2, \ldots, 18 \tag{1-1}$$

To consider the connection between equipment items among each cycle, three evaporators in the first cycle are assumed to exist in the second cycle. Accordingly, the number of equipment in the second cycle is 26, as shown in Table 2.

For the second cycle

$$\Sigma_{k=1}^{5} V_{ik}=1 \quad i=1, 2, \ldots, 26 \tag{1-2}$$

Each equipment item can be located at any floor, occupying only a single floor.

If the height of the equipment exceeds the height of a floor (H=10 m), the equipment is continuously allocated on the floors in the direction of the height. Therefore, the following formulation must be satisfied [19].

For the first cycle

$$\Sigma_{k=1}^{2} V_{1k}V_{2k+1}V_{3k+2}=1 \tag{1-3}$$

$$\Sigma_{k=1}^{2} V_{4k}V_{5k+1}V_{6k+2}=1 \tag{1-4}$$

$$\Sigma_{k=1}^{2} V_{4k}V_{5k+1}V_{6k+2}=1 \tag{1-5}$$

For the second cycle

$$\Sigma_{k=1}^{2} V_{1k}V_{2k+1}V_{3k+2}=1 \tag{1-6}$$

$$\Sigma_{k=1}^{2} V_{4k}V_{5k+1}V_{6k+2}=1 \tag{1-7}$$

$$\Sigma_{k=1}^{2} V_{4k}V_{5k+1}V_{6k+2}=1 \tag{1-8}$$

$$V_{10,1}V_{11,2}V_{12,3}V_{13,4}V_{14,5}=1 \tag{1-9}$$

$$V_{15,1}V_{16,2}V_{17,3}V_{18,4}V_{19,5}=1 \tag{1-10}$$

To avoid situations where two pieces of equipment, i and j, occupy the same physical location, when allocated to the same floor (i. e., $Z_{ij}=1$), appropriate constraints should be included in the model that prohibit the overlapping of their equipment footprint projections in either the x or y direction.

The value of the Z_{ij} variables can be obtained by:

$$Z_{ij} \geq V_{ik}+V_{jk}-1 \quad \forall i=1, \ldots, N-1, j=i+1, \ldots, N, k=1, \ldots, K \tag{2}$$

$$Z_{ij} \geq 1-V_{ik}+V_{jk} \quad \forall i=1, \ldots, N-1, j=i+1, \ldots, N, k=1, \ldots, K \tag{3}$$

$$Z_{ij} \geq 1+V_{ik}-V_{jk} \quad \forall i=1, \ldots, N-1, j=i+1, \ldots, N, k=1, \ldots, K \tag{4}$$

where i=1, 2, …, 17, j=i+1, …, 18, k=1, 2, …, 4 (the first cycle), i=1, 2, …, 25, j=i+1, …, 26, k=1, 2, …, 5 (the second cycle).

Note that if two equipment items, i and j, are allocated to the same floor, then the corresponding Z_{ij} variable is forced to one by constraints (2), whereas constraints (3) and (4) are inactive. In contrast, if equipment i and j are allocated to different floors, then constraints (2) are inactive, whereas constraints (3) and (4) are active and force the Z_{ij} variable to zero.

The length and the depth of i^{th} equipment are determined by the equipment orientation decisions. The effect of the equipment orientation is captured as follows:

$$l_i=\alpha_i O_i+\beta_i(1-O_i) \quad \forall i \tag{5}$$

For the first cycle

$$l_i=\alpha_i O_i+\beta_i(1-O_i) \quad i=1, 2, \ldots, 18 \tag{5-1}$$

For the second cycle

$$l_i=\alpha_i O_i+\beta_i(1-O_i) \quad i=1, 2, \ldots, 26 \tag{5-2}$$

$$d_i=\alpha_i+\beta_i-l_i \quad \forall i \tag{6}$$

For the first cycle

$$d_i=\alpha_i+\beta_i-l_i \quad i=1, 2, \ldots, 18 \tag{6-1}$$

For the second cycle

$$d_i=\alpha_i+\beta_i-l_i \quad i=1, 2, \ldots, 26 \tag{6-2}$$

where O_i is the binary parameter, deciding the equipment length and depth. If O_i is 1, then the equipment length l_i is equal to the equipment dimension α_i or β_i. Moreover, the dimensions of the equipment are shown in Tables 1 and 2.

2-2. Distance Constraints

All the connections between the equipment can be possible through the geometry center of the equipment, as shown Fig. 2. The rectilinear distance was introduced to consider more realistic piping costs. The total rectilinear distance between equipment i and j, TD_{ij}, is determined by considering their relative distances in the x and y coordinates.

The single-floor distance constraints presented by Papageorgiou and Rotstein [11] are here extended for the multifloor case.

$$R_{ij}-L_{ij}=x_i-x_j \quad \forall i=1, \ldots, N-1, j=i+1, \ldots, N \tag{7}$$

$$A_{ij}-B_{ij}=y_i-y_j \quad \forall i=1, \ldots, N-1, j=i+1, \ldots, N \tag{8}$$

$$U_{ij}-D_{ij}=H\Sigma_{k=1}^{NF} k(V_{ik}-V_{jk}) \quad \forall i=1, \ldots, N-1, j=i+1, \ldots, N \tag{9}$$

When equipment i and j are connected, the number of the floors (NF) is equal to 4 (the first cycle), 5 (the second cycle), and the height (H) between the decks is 10 m. The connections of the equipment in each cycle are shown in Tables 3 and 4.

Thus, the total rectilinear distance between equipment i and j is presented by:

Table 3. Connections between equipment in the first cycle of the DMR liquefaction cycle process

No.	From equipment i to equipment j	No.	From equipment i to equipment j
1	8 to 12	10	14 to 5
2	12 to 8	11	5 to 8
3	8 to 16	12	5 to 11
4	16 to 17	13	11 to 5
5	17 to 18	14	5 to 17
6	18 to 15	15	2 to 10
7	15 to 13	16	10 to 2
8	13 to 1	17	2 to
9	2 to 14		

Table 4. Connections between equipment in the second cycle of the DMR liquefaction cycle process

No.	From equipment i to equipment j	No.	From equipment i to equipment j
1	26 to 24	9	17 to 21
2	24 to 23	10	21 to 17
3	23 to 3	11	17 to 12
4	3 to 6	12	12 to 25
5	6 to 9	13	25 to 26
6	8 to 22	14	11 to 20
7	22 to 12	15	20 to 11
8	12 to 17		

$$TD_{ij}=R_{ij}+L_{ij}+A_{ij}+B_{ij}+U_{ij}+D_{ij}$$
$$\forall i=1,\ldots,N-1,\ j=i+1,\ldots,N \tag{10}$$

As previously mentioned, if the height of the equipment exceeds the height of a floor (H=10 m), the equipment is continuously allocated on the floors in the direction of the height. Therefore, the following formulation must be satisfied [19].

For the first cycle

$$x_i=x_{i+1}\quad i=1,2,\ldots,9 \tag{11}$$

$$y_i=y_{i+1}\quad i=1,2,\ldots,9 \tag{12}$$

For the second cycle

$$x_i=x_{i+1}\quad i=1,2,\ldots,19 \tag{13}$$

$$y_i=y_{i+1}\quad i=1,2,\ldots,19 \tag{14}$$

2-3. Nonoverlapping Constraints

To avoid situations where two equipment i and j occupy the same physical location, when allocated to the same floor, appropriate constraints should be included in the model that prohibit overlapping of their equipment footprint projections, either in the x or y direction. Moreover, each equipment item that is allocated on the same floor should avoid overlapping against each other. For this, two binary parameters, $E1_{ij}$, and $E2_{ij}$, and one appropriate upper bound, M, are introduced. The combination of $E1_{ij}$ and $E2_{ij}$ makes the following equations active (Symbols x and y stand for the geometrical center of each equipment).

$$x_i-x_j+M(1-Z_{ij}+E1_{ij}+E2_{ij})\geq\frac{l_i+l_j}{2}$$
$$\forall i=1,\ldots,N-1,\ j=i+1,\ldots,N \tag{15}$$

$$x_j-x_i+M(2-Z_{ij}-E1_{ij}+E2_{ij})\geq\frac{l_i+l_j}{2}$$
$$\forall i=1,\ldots,N-1,\ j=i+1,\ldots,N \tag{16}$$

$$y_i-y_j+M(2-Z_{ij}+E1_{ij}-E2_{ij})\geq\frac{d_i+d_j}{2}$$
$$\forall i=1,\ldots,N-1,\ j=i+1,\ldots,N \tag{17}$$

$$y_j-y_i+M(3-Z_{ij}-E1_{ij}-E2_{ij})\geq\frac{d_i+d_j}{2}$$
$$\forall i=1,\ldots,N-1,\ j=i+1,\ldots,N \tag{18}$$

where M is an appropriate upper bound, and, i=1, 2, …, 17, j=i+1, …, 18, (the first cycle), i=1, 2, …, 25, j=i+1, …, 26 (the second cycle).

Note that the above constraints are inactive for the equipment allocated to different floors, when Z_{ij} is equal to zero.

The lower bound constraints on the coordinates of the geometrical center are included to avoid the intersection of items with the origin of axes:

$$x_i\geq\frac{l_i}{2}\quad\forall i \tag{19}$$

$$y_i\geq\frac{d_i}{2}\quad\forall i \tag{20}$$

where i=1, 2, …, 18 (the first cycle), i=1, 2, …, 26 (the second cycle).

A rectangular shape of the land area was assumed to be used, and its dimensions were determined by the following equations:

$$x_i+\frac{l_i}{2}\leq X^{max}\quad\forall i \tag{21}$$

$$y_i+\frac{d_i}{2}\leq Y^{max}\quad\forall i \tag{22}$$

where i=1, 2, …, 18 (the first cycle), i=1, 2, …, 26 (the second cycle).

These dimensions were then used to calculate the land area (FA):

$$FA=X^{max}Y^{max} \tag{23}$$

2-4. Objective Function

The objective function is defined as follows, minimizing the sum of the cost of pipe connection, pumping (vertical and horizontal), floor construction, land, and area dependent land:

$$\text{Min.}\Sigma_i^N\Sigma_{j\neq i/f_{ij}}[C_{ij}^cTD_{ij}+C_{ij}^vD_{ij}+C_{ij}^h(R_{ij}+L_{ij}+A_{ij}+B_{ij})]$$
$$+FC1\cdot NF+FC2\cdot NF\cdot FA+LC\cdot FA \tag{24}$$

where C_{ij}^c is the connection cost between equipment i and j, C_{ij}^v is the vertical pumping cost between equipment i and j, FCl is the fixed floor construction cost, FC2 is the area dependent floor construction cost, and LC is the land cost.

Because Eq. (24) is nonlinear, the following equations are added to maintain the entire problem as an MILP:

$$FA=\Sigma_sAR_sQ_s \tag{25}$$

$$\Sigma_sQ_s=1 \tag{26}$$

$$NQ_s\leq K\cdot Q_s\quad\forall s \tag{27}$$

$$NF=\Sigma_sNQ_s \tag{28}$$

where AR_s is the parameter for the candidate area list, and NQ_s is an integer variable for the number of floors. Then, the objective function is rewritten as follows:

$$\text{Min.}\Sigma_i^N\Sigma_{j\neq i/f_{ij}}^N[C_{ij}^cTD_{ij}+C_{ij}^vD_{ij}+C_{ij}^h(R_{ij}+L_{ij}+A_{ij}+B_{ij})]$$
$$+FC1\cdot NF+FC2\cdot\Sigma_sAR_s\cdot NQ_s+LC\cdot FA \tag{29}$$

In the DMR liquefaction cycle process, there are high-pressure systems using compressors, and pumps are not used in our study. The number of floors for each process is fixed in our study. Thus, the floor construction cost is not required as an objective function. In

conclusion, in our study the objective function used is shown in Eq. (30). In addition, the LC value was assumed to have a very high value than the connection cost.

$$\text{Min.}\Sigma_i^N\Sigma_{j\neq i/f_{ij}}^N[C_{ij}^c TD_{ij}]+LC\cdot FA \quad (30)$$

subject to constraints Eqs. (1)-(22) and Eqs. (25)-(28).

COMPUTATIONAL RESULTS AND DISCUSSION

In this section, the proposed approach is applied to the generic LNG liquefaction process plant presented above. The optimal multifloor layout for the DMR LNG liquefaction cycle process was obtained using the GAMS modeling system coupled to the CPLEX MILP optimization package. To minimize the disconnection between equipment and equipment among each part, an optimization was performed by dividing into the first and the second cycles. As shown in Fig. 2, three evaporators in the first cycle are connected to the second cycle. Therefore, for satisfying the distance constraint between the equipment among each cycle, and optimizing the distance constraint for the entire process, the three evaporators were assumed to be in the first cycle in the second cycle.

1. First Cycle Process Plant

The dimensions of all the equipment for the first cycle of the generic LNG liquefaction process plant are listed in Table 1. To perform the optimal plant layout of the first cycle processes plants, the height between the floors was assumed to be 10 m, and the number of floors NF=4. For the safety of the process, the minimum distance between the equipment was assumed to be 3 m. Therefore, Eqs. (19)-(22) of the nonoverlapping constraints can be derived as follows.

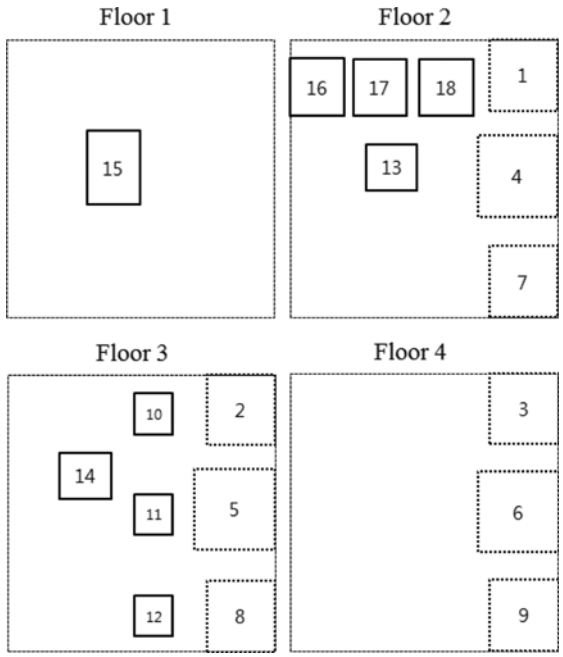

Fig. 3. Optimal layout for the first cycle of the DMR liquefaction process.

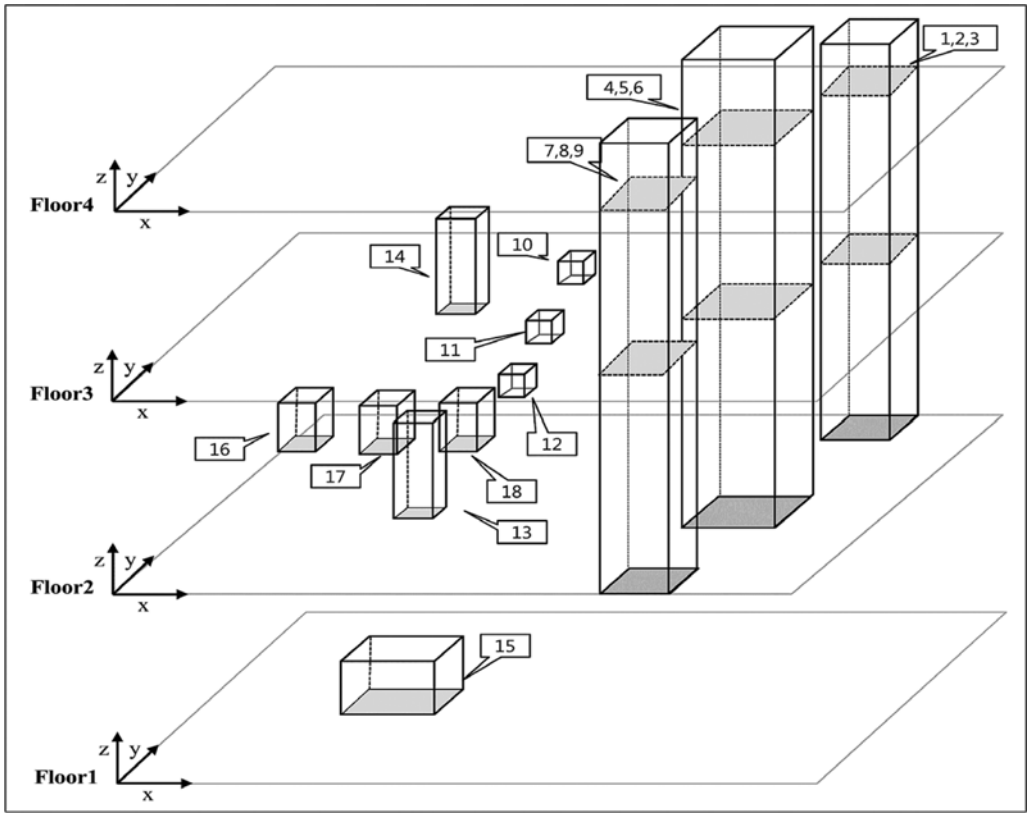

Fig. 4. 3D view for the first cycle of the DMR liquefaction process.

$$x_i \geq \frac{l_i}{2} + 3 \quad \forall i \tag{31}$$

$$y_i \geq \frac{d_i}{2} + 3 \quad \forall i \tag{32}$$

where i=1, 2, …, 18 (the first cycle), i=1, 2, …, 26 (the second cycle)

A rectangular shape of the land area was assumed to be used, and its dimensions were determined by the following equations:

$$x_i + \frac{l_i}{2} + 3 \leq X^{max} \quad \forall i \tag{33}$$

$$y_i + \frac{d_i}{2} + 3 \leq Y^{max} \quad \forall i \tag{34}$$

where i=1, 2, …, 18 (the first cycle), i=1, 2, …, 26 (the second cycle)

The resulting mathematical model includes 725 continuous variables, 198 equality constraints, and 1,107 inequality constraints. The required computing time is 18.2 CPU seconds on Intel (R) Core (TM) i7-2670QM CPU 2.2.GHz. The optimal multifloor process layout of the first cycle is shown in Figs. 3 and 4. The optimal solution (equipment location, equipment-floor allocation) is provided in Table 5. The optimal land area of each floor is 475 m^2 (X^{max}=25, Y^{max}=19).

Table 5. Optimal solution for the first cycle of the DMR liquefaction cycle process

No.	Name of equipment	Allocation		Allocation floor
		x_i (m)	y_i (m)	
1	Evaporator 1 (floor 2)	23	17	2
2	Evaporator 1 (floor 3)	23	17	3
3	Evaporator 1 (floor 4)	23	17	4
4	Evaporator 2 (floor 2)	22.5	9.5	2
5	Evaporator 2 (floor 3)	22.5	9.5	3
6	Evaporator 2 (floor 4)	22.5	9.5	4
7	Evaporator 3 (floor 2)	23	2	2
8	Evaporator 3 (floor 3)	23	2	3
9	Evaporator 3 (floor 4)	23	2	4
10	Expansion valve 1	18.5	17	3
11	Expansion valve 2	18.5	9.5	3
12	Expansion valve 3	18.5	2	3
13	Phase separator 1	11	10	2
14	Phase separator 2	13	11	3
15	Condenser	11	10	1
16	Compressor 1	2	16	2
17	Compressor 2	9	16	2
18	Compressor 3	16	16	2

2. Second Cycle Process Plant

The dimensions of all the equipment for the second cycle process plant are listed in Table 2. To perform the optimal plant layout of the second cycle process plants, the height between the floors was assumed to be 10 m, and NF=5. For the safety of the process, the minimum distance between the equipment was assumed to be 3 m. Thus, Eqs. (31)-(34) were applied for the second cycle process plant layout.

The resulting mathematical model includes 1,291 continuous variables, 286 equality constraints, and 2,327 inequality constraints. To solve the optimal solution, the required computing time is 28.9 CPU seconds. The optimal multifloor process layout of the second cycle is shown in Fig. 5, and Fig. 6 is the 3D view, excluding three evaporators in the first cycle for the second cycle of the DMR liquefaction process. The optimal solution is listed in Table 6. Moreover, the optimal land area of each floor was 500 m^2 (X^{max}=20, Y^{max}=

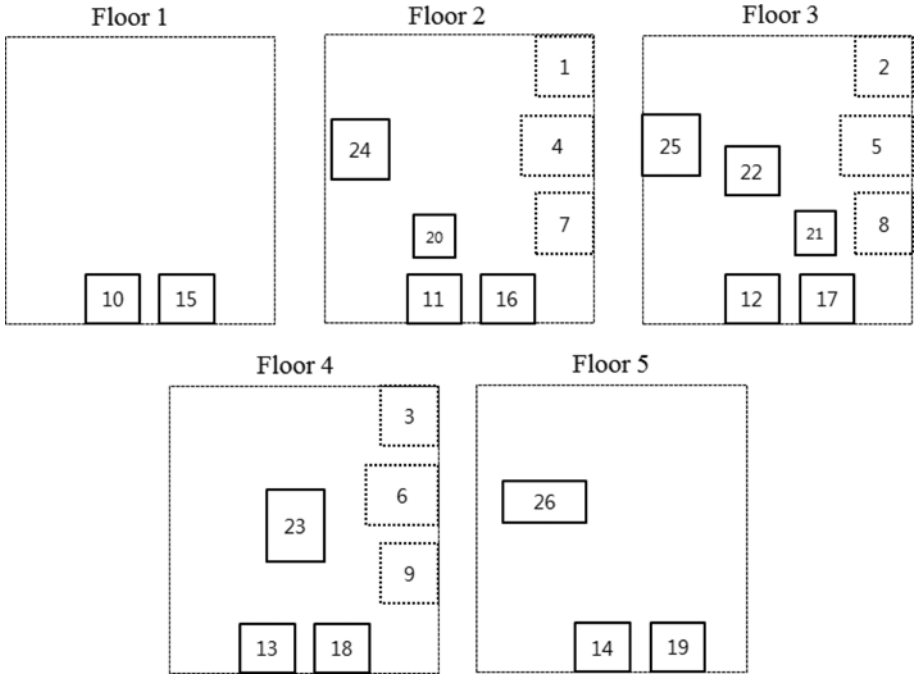

Fig. 5. Optimal layout for the second cycle of the DMR liquefaction process.

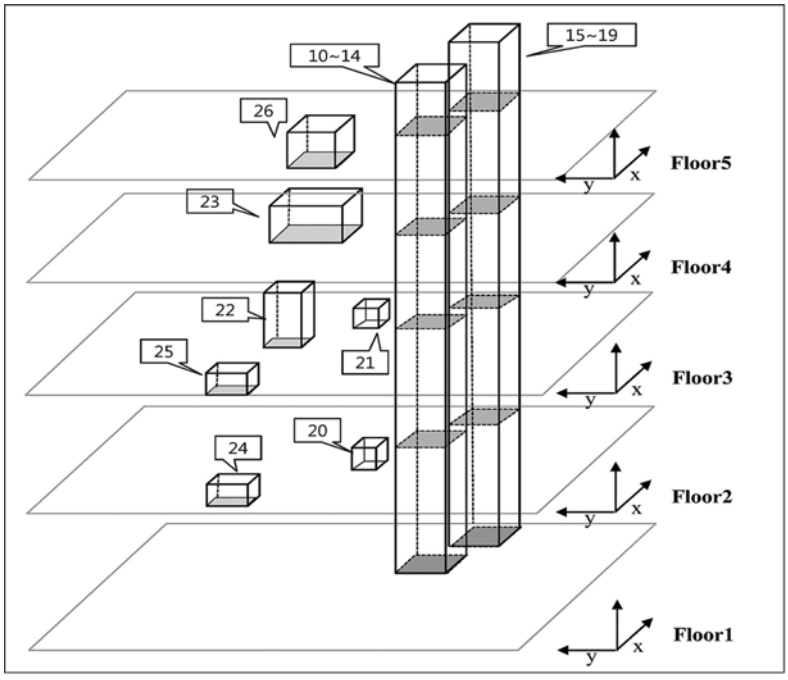

Fig. 6. 3D view for the second cycle of the DMR liquefaction process.

Table 6. Optimal solution for the second cycle of the DMR liquefaction cycle process

No.	Name of equipment	Allocation		Allocation floor
		x_i (m)	y_i (m)	
1	Evaporator 1 (first cycle)	18	23	2
2	Evaporator 1 (first cycle)	18	23	3
3	Evaporator 1 (first cycle)	18	23	4
4	Evaporator 2 (first cycle)	17.5	15.5	2
5	Evaporator 2 (first cycle)	17.5	15.5	3
6	Evaporator 2 (first cycle)	17.5	15.5	4
7	Evaporator 3 (first cycle)	18	8	2
8	Evaporator 3 (first cycle)	18	8	3
9	Evaporator 3 (first cycle)	18	8	4
10	Evaporator 1 (second cycle)	8.5	1.5	1
11	Evaporator 1 (second cycle)	8.5	1.5	2
12	Evaporator 1 (second cycle)	8.5	1.5	3
13	Evaporator 1 (second cycle)	8.5	1.5	4
14	Evaporator 1 (second cycle)	8.5	1.5	5
15	Evaporator 2 (second cycle)	14.5	1.5	1
16	Evaporator 2 (second cycle)	14.5	1.5	2
17	Evaporator 2 (second cycle)	14.5	1.5	3
18	Evaporator 2 (second cycle)	14.5	1.5	4
19	Evaporator 2 (second cycle)	14.5	1.5	5
20	Expansion valve 1	8.5	6.5	2
21	Expansion valve 2	12.5	6.5	3
22	Phase separator 1	8.5	11.5	3
23	Condenser	10	13	4
24	Compressor 1	2	13	2
25	Compressor 2	2	13	3
26	Intercooler 1	7	14	5

25). However, for satisfying the distance constraint between equipment and considering the connection between the equipment among each cycle, three evaporators in the first cycle were assumed to exist in the second cycle. Therefore, if the three virtual evaporators are excluded, the actual optimal land area was 240 m^2 (X^{max}=15, Y^{max}=16).

In this study, the optimal multifloor process plant layout problem of the generic offshore LNG liquefaction plant for the DMR cycle was considered. The optimization of the plant layout was performed based on the MILP model, proposed by Patsiatzis and Papageorgiou [14]. The results of this study will help to reduce the area cost occupied by the generic offshore LNG liquefaction plant at the front-end engineering design stage. For future study, the optimal multifloor layout considering the safety such as physical explosions, vapor cloud explosions, and boiling liquid expanding vapor explosions will be considered. Moreover, the proposed method will be applied to the optimal multifloor layout of the various floating offshore.

NOMENCLATURE

Indices

i, j : equipment item
k : floor
s : candidate area

Parameters

α_i, β_i : dimensions of item i
H : floor height
f_{ij} : 1, if flow is from item i to item j; 0, otherwise
C_{ij}^c : connection cost between items i and j
C_{ij}^v : vertical pumping cost between items i and j

C_{ij}^{h} : horizontal pumping cost between items i and j
FC1 : fixed floor construction cost
FC2 : area dependent floor construction cost
LC : land cost

Integer Variables
NF : number of floors

Binary Variables
V_{ik} : 1, if item i is assigned to floor k; 0, otherwise
Z_{ij} : 1, if equipment items i and j are allocated to the same floor; 0, otherwise
O_i : 1, if length of item i is equal to α_i (i.e. parallel to x-axis); 0, otherwise
$E1_{ij}$, $E2_{ij}$: non-overlapping binary variables (as used in Papageorgiou and Rotstein, 1998)

Continuous Variables
l_i : length of item i
d_i : depth of item i
x_i, y_i : coordinates of geometrical center of item i
R_{ij} : relative distance in x coordinates between items i and j, if i is to the right of j
L_{ij} : relative distance in x coordinates between items i and j, if i is to the left of j
A_{ij} : relative distance in y coordinates between items i and j, if i is above j
B_{ij} : relative distance in y coordinates between items 1 i and j, if i is below j
U_{ij} : relative distance in z coordinates between items i and j, if i is higher than j
D_{ij} : relative distance in z coordinates between items i and j, if i is lower than j
TD_{ij} : total rectilinear distance between items i and j
FA : floor area
X^{max}, Y^{max} : dimensions of floor area

REFERENCES

1. J. H. Hwang, M. I. Roh and K. Y. Lee, *Comput. Chem. Eng.*, **49**, 25 (2013).
2. J. H. Hwang, N. L. Ku, M. I. Roh and K. Y. Lee, *Ind. Eng. Chem. Res.*, **52**, 5341 (2013).
3. W. Lim, K. Choi and I. Moon, *Ind. Eng. Chem. Res.*, **52**, 3065 (2013).
4. S. Lee, N. V. D. Long and M. Lee, *Ind. Eng. Chem. Res.*, **51**, 10021 (2012).
5. L. Amorese, V. Cena and C. Mustacchi, *Chem. Eng. Sci.*, **32**, 119 (1991).
6. M. C. Georgiadis, G. E. Rotstein and S. Macchietto, *Ind. Eng. Chem. Res.*, **36**, 4852 (1997).
7. M. C. Georgiadis, G. Schilling, G. E. Rotstein and S. Macchietto, *Comput. Chem. Eng.*, **23**, 823 (1999).
8. S. Jayakumar and G. V. Reklaitis, *Comput. Chem. Eng.*, **14**, 441 (1994).
9. S. Jayakumar and G. V. Reklaitis, *Comput. Chem. Eng.*, **20**, 563 (1996).
10. C. M. L. Castell, R. Lakshmanan, J. M. Skilling and R. Bañares-Alcàntara, *Comput. Chem. Eng.*, **22S**, S993 (1998).
11. L. G. Papageorgiou and G. E. Rotstein, *Ind. Eng. Chem. Res.*, **37**, 3631 (1998).
12. F. D. Penteado and A. R. Ciric, *Ind. Eng. Chem. Res.*, **35**, 1354 (1996).
13. A. Suzuki, T. Fuchino and M. Muraki, *J. Chem. Eng. Japan*, **24**, 226 (1991).
14. D. I. Patsiatzis and L. G. Papageorgiou, *Comput. Chem. Eng.*, **26**, 575 (2002).
15. D. I. Patsiatzis G. Knight and L. G. Papageorgiou, *Chem. Eng. Res. Design*, **82**, 579 (2004).
16. K. Park, J. Koo, D. Shin, C. J. Lee and E. S. Yoon, *Korean J. Chem. Eng.*, **28**(4), 1009 (2011).
17. D. B. Ozyruth and M. J. Realff, *AIChE J.*, **45**, 2161 (1999).
18. T. Shukri, LNG Technology Selection, Hydrocarbon Engineering, USA (2004).
19. N. K. Ku, J. H. Hwang, J. C. Lee, M. I. Roh and K. Y. Lee, *Ships and Offshore Structure*, **9**, 311 (2014).
20. J. H. Hwang and K. Y. Lee, *Comput. Chem. Eng.*, **63**, 1 (2014).
21. W. Won, S. K. Lee, K. Choi and Y. Kwon, *Korean J. Chem. Eng.*, **31**(5), 732 (2014).